VOLUME 111, NUMBER 7
MARCH 29, 1989

JOURNAL
OF THE
AMERICAN
CHEMICAL
SOCIETY

Covalency in Bis([8]annulene)uranium from Photoelectron Spectroscopy with Variable Photon Energy

John G. Brennan, Jennifer C. Green,* and Catherine M. Redfern

Contribution from the Inorganic Chemistry Laboratory, University of Oxford, South Parks Road, Oxford OX1 3QR, England. *Received June 28, 1988*

Abstract: Relative partial photoionization cross sections and photoelectron branching ratios of the valence bands (6–22-eV binding energy) of bis([8]annulene)uranium(IV) are reported over the photon energy range 24–125 eV. The f^{-1} band shows cross-section features attributable to 5f resonant photoemission in the vicinity of the 5d → 5f giant resonant absorption ($h\nu$ = 101 and 110 eV). The e_{2g}^{-1} and e_{2u}^{-1} bands also show small cross-section maxima at these energies, that for the e_{2u}^{-1} ionization being the more intense. The f^{-1} band shows a large maximum at 39 eV, which is assigned to a delayed maximum due to the centrifugal barrier. The three highest ionization energy bands (from ligand-based orbitals) show essentially monotonic cross section decrease with photon energy. The mapping of the intensity changes of the f^{-1} band by the e_{2u}^{-1} band provides strong evidence for f orbital covalency in this molecule.

Covalent contributions to the stability of organoactinide molecules have been widely debated[1] ever since the first reported preparation of an organouranium complex.[2] Electronic structure elucidation in 5f metal chemistry is hampered by the extreme complexity of the properties ascribable to 5f electrons, and conventional means of electronic structure characterization such as optical spectroscopy, magnetic susceptibility,[3] or NMR spectroscopy[4] currently yield uninterpretable data in all but the most symmetric cases. Even in the most favorable cases, most evidence related to the properties of the f electrons themselves, whereas orbitals influenced by f orbital covalency are likely to be more low-lying, largely ligand-based, and less accessible by these techniques.

Photoelectron spectroscopy (PES) remains one of the more useful means of electronic structure characterization in organoactinide chemistry, as the data are not overwhelmed by the complex nature of the f electrons and this technique is able to probe selectively the lower lying molecular levels. The empirical interpretation of relative He I/He II band intensities have been used as evidence for both d and f orbital covalency in molecules such as $(C_5H_4R)_4U$ (R = H[5] and CH_3[6] and $U(OMe)_6$.[7] One of the most convincing spectroscopic arguments for covalency in actinide complexes is the analysis of the photoelectron (PE) spectra of bis([8]annulene)uranium (uranocene) and thorium,[8-10] where the relative intensity increase in one ligand band suggested a substantial ligand–f orbital covalent interaction. Unfortunately, relative intensity changes in He I/He II spectra are not unequivocal evidence for metal character in a photoelectron band.

* Author to whom correspondence should be addressed.

(1) (a) Marks, T. J., Fischer, R. D., Eds. *Organometallics of the f-elements*; Reidel: Dordrecht, Holland, 1979. (b) Marks, T. J.; Ernst, R. D. In *Comprehensive Organometallic Chemistry*; Wilkinson, G., Stone, F. G. A., Abel, E. W., Eds.; Pergamon Press: Oxford, England, 1982. (c) Marks, T. J. *Prog. Inorg. Chem.* **1979**, *25*, 224. (d) Raymond, K. N.; Eigenbrot, C. W., Jr. *Acc. Chem. Res.* **1980**, *13*, 276. (e) Bursten, B. E.; Strittmatter, R. J. *J. Am. Chem. Soc.* **1987**, *109*, 6606.
(2) Reynolds, L. T., Wilkinson, G. *J. Inorg. Nucl. Chem.* **1956**, *2*, 246.
(3) Gamp, E.; Shinomoto, R.; Edelstein, N.; McGarvey, B. R. *Inorg. Chem.* **1987**, *26*, 2177 and references therein.
(4) Rajnak, K.; Gamp, E.; Shinomoto, R.; Edelstein, N. *J. Chem. Phys.* **1984**, *80*, 5942 and references therein.
(5) Green, J. C.; Kelley, M. R.; Long, J. A.; Kanellakopulos, B.; Yarrow, P. I. W. *J. Organomet. Chem.* **1981**, *212*, 329.
(6) Bursten, B. E.; Casarin, M.; DiBella, S.; Fang, A.; Fragala, I. L. *Inorg. Chem.* **1985**, *24*, 2169.
(7) Bursten, B. E.; Casarin, M.; Ellis, D. E. A.; Fragala, I. L.; Marks, T. J. *Inorg. Chem.* **1986**, *25*, 1257.
(8) Clark, J. P.; Green, J. C. *J. Organomet. Chem.* **1976**, *112*, C14.
(9) Fragala, I. L.; Condorelli, G.; Zanella, P.; Tondello, E. *J. Organomet. Chem.* **1976**, *122*, 357.
(10) Clark, J. P.; Green, J. C. *J. Chem. Soc., Dalton Trans.* **1977**, 505.

0002-7863/89/1511-2373$01.50/0

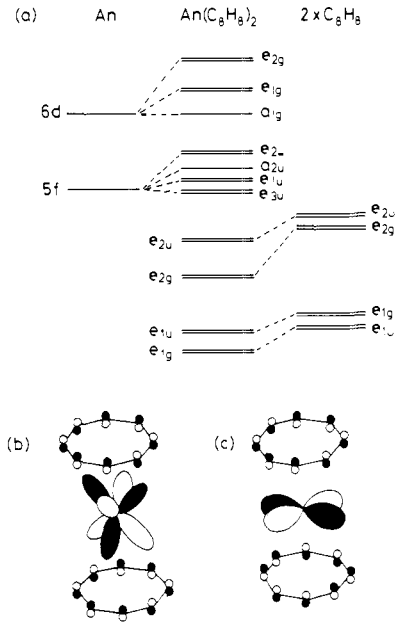

Figure 1. (a) Schematic MO diagram for an actinocene with D_{8h} symmetry, (b) interaction of f orbital with the ligand e_{2u} orbital, (c) interaction of a d orbital with the ligand e_{2g} orbital.

As well as different percentages of atomic character, multielectron processes or configuration interactions can also have a significant effect on relative intensity changes in the 20–40-eV energy range used by conventional photoelectron spectroscopists.

The energy dependence of photoionization cross sections reveals a great deal of information on electronic structure. Synchrotron radiation allows an extensive range of photon energies to be used in photoelectron experiments, illuminating the foundations and limitations of empirical intensity rules based on He I/He II[11,12] differences. Use of an angle-resolved gas-phase PE spectrometer at Daresbury[13] has afforded us the opportunity of carrying out PES on gas-phase transition-metal compounds over a wide photon energy range. Experiments on $M(CO)_6$ (M = Cr, Mo, and W)[14] and $M(\eta^2\text{-}C_5H_5)_2$ (M = Fe, Ru, and Os)[15] reveal significant differences in behavior between metal and ligand cross-section behavior. Relative partial photoionization cross sections (RPPICS) of the ligand bands are mainly characterized by a rapid decline with increasing photon energy, whereas RPPICS of the metal bands show a slower decrease with photon energy and a wealth of features.

Following the success of these studies on the d block transition metals, we extended the study to the f series. Uranocene is a high-symmetry (D_{8h}) molecule whose bonding can be treated in a similar fashion to that of the d block metallocenes (see Figure 1). In actinocene complexes the e_{2u} orbital can be a bonding level as the central atom possesses low-lying 5f orbitals of e_{2u} symmetry. Hence, a study of this kind of uranocene enables us to look at the behavior of bands of metal f, ligand, and mixed metal/ligand character.

Initial assignment of the e_{2u} and e_{2g} bands in the uranocene He I PE spectrum[8,9] was superceded by a reversal in assignment upon acquisition of the He II PE spectrum,[10] with the first ligand band attributed to the e_{2u} orbital. Two facets of the uranocene PE spectra provided important data concerning structure and bonding in actinide organometallics. First, the substantial increase in relative intensity of the e_{2u} band using He II radiation suggested a significant e_{2u}–f orbital covalent interaction, and second, the relative stability of the e_{2g} orbital with respect to the e_{2u} orbital was evidence for strong e_{2g}–6d bonding. Numerous theoretical calculations[16-19] have supported this PE assignment, but given the numerous possible explanations for relative intensity changes, as unequivocal assignment based on thorough characterization with synchrotron light would seem desirable.

Experimental Section

A full account of our experimental method has been given[14] and the apparatus and its performance is described elsewhere,[13] therefore only a brief account of experimental procedures is given here.

Synchrotron radiation from the 2-GeV electron storage ring at SERC Daresbury Laboratory was monochromated using a toroidal grating monochromator (TGM) and was used to photoionize gaseous samples in a cylindrical ionization chamber. The TGM was employed with fixed slit widths of 2 mm. Total instrumental resolution was monochromator limited and was in the range 50–300 meV. The photoelectrons were energy analyzed with a three-element zoom lens in conjunction with a hemispherical electron energy analyzer, which was positioned at the "magic angle" in order to eliminate the influence of the photoelectron asymmetry parameter, β, on signal intensity. This angle is dependent on the polarization of the radiation and varies with photon energy. The polarization varied from 67–88%, and the magic angle for each uranocene and inert-gas spectrum was adjusted accordingly. The magic angle used varied from 120.1–123.8°. Multiple-scan PE spectra were collected at each photon energy required. The decay of the storage ring beam current was corrected for by linking the scan rate with the output from a photodiode positioned to intersect the photon beam after it had passed through the gas cell. The sensitivity of the photodiode to different radiation energies was determined by measuring the np^{-1} PE spectra of Ne, Ar, and Xe. These were also used to characterize and correct for a falloff in analyzer collection efficiency at kinetic energies $\leq$ 15 eV. Photoionization cross sections for the rare gases were taken from the literature.[20,21]

The sample, introduced into the chamber in a naphthalene plugged tube, was sublimed into the gas cell by heating with Semflex noninductively wound heating wire. A liquid nitrogen cooled cold finger collected the used sample. Pressure fluctuations of the sample were corrected for by collecting a "standard" calibration spectrum before and after each data spectrum. The intensities of the bands in these spectra were then used as a relative measure of the sample density in the ionization region.

Uranocene was prepared by reating $K_2(C_8H_8)$ with UCl_4 according to standard literature procedures[22] but was then isolated by washing the reaction mixture with H_2O (to remove KCl and any unreacted starting materials) and heating under vacuum to remove trace volatiles. Purity was established by comparing its He I spectrum, obtained on a PES Laboratories 0078 spectrometer, with literature reports.[8-10]

Data Analysis

The branching ratio (BR) data are independent of the sensitivity of the photodiode to photon energy and the long-term variation in sample pressure and are only corrected with the kinetic energy calibration. The three bands of particular interest in this study (f, e_{2u}, and e_{2g}) have a kinetic energy of greater than 15 eV at all photon energies studied so no corrections have been applied to their branching ratios. For the points on the RPPICS plots, where pressure variations and photodiode calibration factors also contribute to the possible errors, relative values of points within 5 eV of each other are probably accurate to within 5%, whereas data separated by >20 eV contain a relative uncertainty of 10%. All RPPICS features commented upon and discussed below are also clearly visible in the BR plots.

Where bands were clearly separated, their areas were determined by integration after subtraction of a linear background. However, at higher photon energies the f^{-1}, e_{2g}, and e_{2u} bands overlap strongly. Three methods used to deconvolute these three bands were integration and fitting of both symmetric and asym-

(11) Price, W. C.; Potts, A. W.; Streets, D. G. In *Electron Spectroscopy*; Shirley, D. A., Ed.; North-Holland: Amsterdam, Holland, 1972; p 187.
(12) Green, J. C. *Struct. Bonding* **1981**, *43*, 37.
(13) Potts, A. W.; Novak, I.; Quinn, F.; Marr, G. V.; Dobson, B. R.; Hillier, I. H. *J. Phys. B* **1985**, *18*, 3177.
(14) Cooper, G.; Green, J. C.; Payne, M. P.; Dobson, B. R.; Hillier, I. H. *J. Am. Chem. Soc.* **1987**, *109*, 3836.
(15) Cooper, G.; Green, J. C.; Payne, M. P. *Mol. Phys.* **1988**, *63*, 1031.
(16) Hayes, R. G.; Edelstein, N. *J. Am. Chem. Soc.* **1972**, *94*, 8688.
(17) Streitweiser, A., Jr.; Muller-Westerhoff, U. *J. Am. Chem. Soc.* **1968**, *90*, 7364.
(18) Rösch, N.; Streitweiser, A., Jr. *J. Am. Chem. Soc.* **1983**, *105*, 7237.
(19) Pyykko, P.; Lohr, L. L. *Inorg. Chem.* **1981**, *20*, 1950.
(20) West, J. B.; Marr, G. V. *Proc. R. Soc. London A* **1976**, *349*, 397.
(21) West, J. B.; Morton, J. *At. Data Nucl. Data Tables* **1978**, *22*, 103.
(22) Streitweiser, A., Jr.; Muller-Westerhoff, U.; Sonnichsen, G.; Mares, F.; Morrell, D. G.; Hodgson, K. O.; Harmon, C. A. *J. Am. Chem. Soc.* **1978**, *95*, 8644.

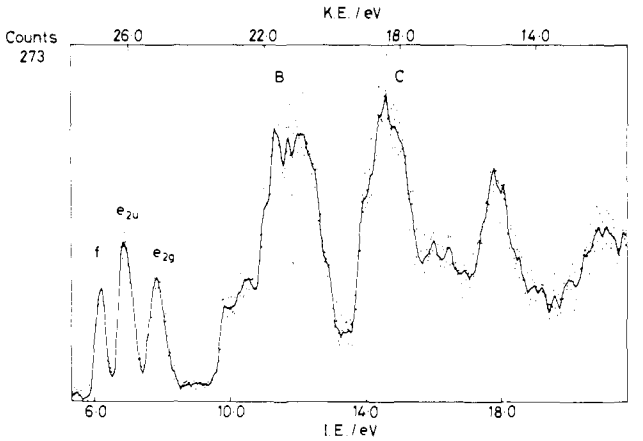

Figure 2. Photoelectron spectrum of uranocene with band labelings taken at a photon energy of 33 eV. The points represent the experimental data, and the solid line represents a least-squares fit to these points.

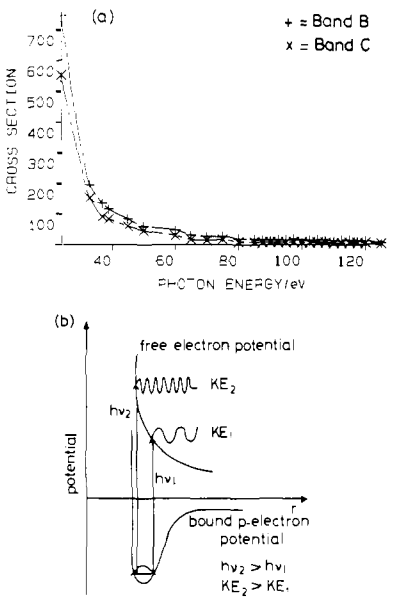

Figure 3. (a) RPPICS of the ligand-based bands B and C, (b) a schematic representation of the decrease in overlap between the free electron wave and the ground-state 2p electronic wave function as the KE of the outgoing electron increases with increasing photon energy.

metric peaks. All three gave the same qualitative results and the RPPICS plots all have the same form. The most reliable method for obtaining the band area was fitting symmetric Gaussian curves to the spectra, the best fit being determined by the method of least squares. The three band positions were fixed relative to each other during the fits and the widths of the e_{2g} and e_{2u} bands were constrained to be equal. All RPPICS presented for these bands are based on band areas obtained by this method. We cannot be sure that complete separation of the e_{2g} and e_{2u} bands is achieved, especially at higher photon energies so some features in the RPPICS and BRs of these two bands may be due to incomplete deconvolution.

Results

A schematic MO diagram for a bis([8]annulene)actinocene is shown in Figure 1. A PE spectrum of the valence region together with band assignments to ionization from the various MO is shown in Figure 2. RPPICS and branching ratios for the valence ionizations of uranocene hve been measured over the energy range 27–130 eV. RPPICS of the ligand-based bands B and C are shown in Figure 3. Valence-band photoelectron branching ratios and RPPICS for the f^{-1}, e_{2u}, and e_{2g} bands of uranocene are shown in Figures 4, 7, and 8 and tabulated in Table I. Experimental uncertainties quoted in Table I originate from statistical errors associated with band area measurements. The relative cross-

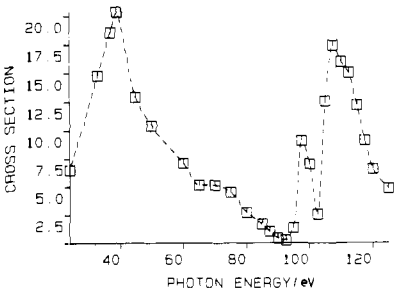

Figure 4. RPPICS of the f band of uranocene.

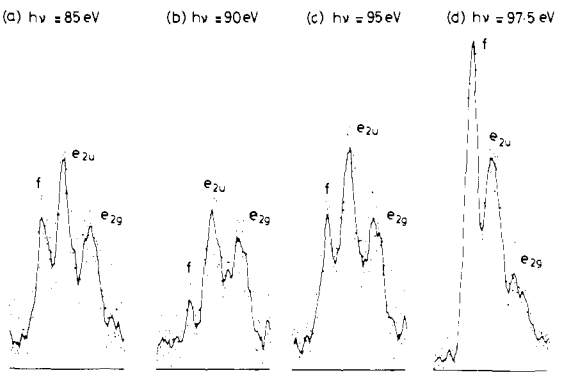

Figure 5. Photoelectron spectra of the f, e_{2u}, and e_{2g} bands of uranocene: (a) $h\nu$ = 85 eV; (b) $h\nu$ = 90 eV; (c) $h\nu$ = 95 eV; (d) $h\nu$ = 97.5 eV. The points represent the experimental data, and the solid line represents a least-squares fit to these points.

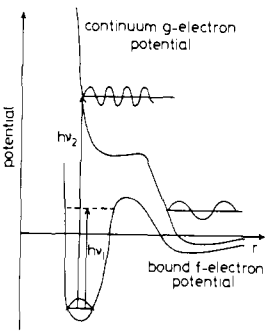

Figure 6. Origin of delayed maximum in the f band RPPICS from the centrifugal barrier in the bound f electron electronic potential.

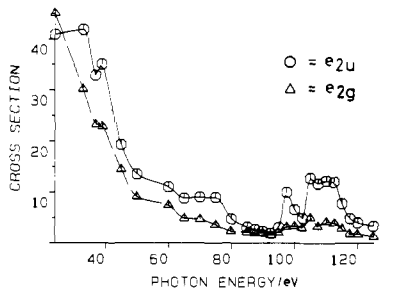

Figure 7. RPPICS of the e_{2u} and e_{2g} bands of uranocene.

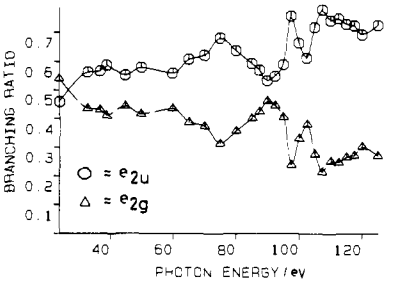

Figure 8. e_{2u}/e_{2g} branching ratios of uranocene.

Table I. RPPICS and BRs for the f, e_{2u}, and e_{2g} Ionizations of Uranocene

	f		e_{2u}		e_{2g}	
$h\nu$	RPPICS	BR	RPPICS	BR	RPPICS	BR
24.0	6.49 ± 0.36	0.005	40.91 ± 1.06	0.021	45.07 ± 1.08	0.025
33.0	15.65 ± 0.51	0.033	41.89 ± 0.96	0.068	30.20 ± 0.79	0.052
37.0	18.57 ± 0.54	0.059	32.89 ± 0.86	0.075	22.31 ± 0.65	0.057
39.0	20.36 ± 0.51	0.072	35.05 ± 0.77	0.090	22.87 ± 0.62	0.063
45.0	12.91 ± 0.28	0.066	19.32 ± 0.41	0.075	14.46 ± 0.33	0.057
50.0	10.42 ± 0.22	0.073	13.51 ± 0.28	0.068	9.06 ± 0.23	0.049
60.0	7.10 ± 0.24	0.076	11.03 ± 0.35	0.086	7.40 ± 0.27	0.067
65.0	5.13 ± 0.14	0.086	8.79 ± 0.22	0.108	4.84 ± 0.15	0.069
70.0	5.13 ± 0.13	0.098	9.05 ± 0.20	0.126	4.70 ± 0.13	0.076
75.0	4.47 ± 0.16	0.086	9.04 ± 0.26	0.128	3.61 ± 0.16	0.059
80.0	2.69 ± 0.08	0.079	4.72 ± 0.11	0.101	2.29 ± 0.08	0.057
85.0	1.67 ± 0.07	0.067	3.09 ± 0.10	0.085	2.09 ± 0.08	0.058
87.5	1.00 ± 0.06	0.035	2.60 ± 0.09	0.091	1.93 ± 0.08	0.067
90.0	0.40 ± 0.03	0.013	2.25 ± 0.07	0.073	1.95 ± 0.07	0.063
92.5	0.23 ± 0.23	0.009	1.88 ± 0.07	0.072	1.52 ± 0.07	0.059
95.0	1.34 ± 0.05	0.044	3.03 ± 0.08	0.099	2.07 ± 0.07	0.068
97.5	9.10 ± 0.15	0.180	9.93 ± 0.16	0.196	3.14 ± 0.09	0.062
100.0	7.03 ± 0.16	0.161	6.57 ± 0.16	0.151	3.27 ± 0.11	0.075
102.5	2.55 ± 0.09	0.081	4.82 ± 0.13	0.152	2.99 ± 0.10	0.094
105.0	12.56 ± 0.24	0.235	12.76 ± 0.24	0.238	4.92 ± 0.15	0.092
107.5	17.44 ± 0.28	0.317	11.66 ± 0.22	0.212	3.24 ± 0.12	0.059
110.0	15.99 ± 0.27	0.298	12.29 ± 0.25	0.229	4.20 ± 0.14	0.078
112.5	12.51 ± 0.24	0.249	10.28 ± 0.22	0.205	3.36 ± 0.12	0.067
115.0	12.22 ± 0.22	0.266	7.77 ± 0.18	0.169	2.85 ± 0.11	0.062
117.5	9.14 ± 0.23	0.248	4.79 ± 0.17	0.130	1.80 ± 0.10	0.049
120.0	6.57 ± 0.13	0.208	3.96 ± 0.10	0.126	1.73 ± 0.07	0.055
125.0	4.81 ± 0.13	0.229	3.27 ± 0.10	0.156	1.23 ± 0.06	0.058

section scales, although in arbitrary units, are internally consistent between plots.

Discussion

A striking difference exists between the cross-section behavior of the electrons having at least some metal character and the electrons associated purely with bonding in the organic portion of the molecule. In uranocene, the d and f orbitals cannot mix by symmetry, and thus deviations in ligand RPPICS behavior from purely C $p\pi$ cross-section behavior can be attributed to either f or d orbital contributions but not both. Attention will focus primarily on the behavior of the metal f, e_{2g}, and e_{2u} orbitals, in an attempt to assess the contributions of f and d orbital covalency to the stability of the complex. For comparative purposes the behavior of the ligand-based orbitals will be established first.

Ligand Bands B + C. Figure 3a shows the RPPICS of the bands associated with the more strongly bound π-electrons and the σ-framework of the uranocene ligand. The cross sections of these bands show an exponential decrease with photon energy similar in behavior to the cross sections of ethylene.[23] Here, the overlap of the outgoing electron wave function with the ground electronic state decreases as the photon energy increases because of its oscillatory nature (see Figure 3b). The ionization dipole matrix elements begin to cancel each other,[24] and consequently the cross section decreases. This featureless cross-section behavior is typical of strongly bound ligand-based orbitals with no metal character.[14,15,23]

f Band. The RPPICS plots of this band are shown in Figure 4 and some typical spectra of the metal and first two ligand bands shown in Figure 5. From the spectra and RPPICS plots we can see that the metal band cross sections are exceedingly sensitive to photon energy. Several interesting features of predominantly atomic origin can be observed in the cross-section behavior of this band.

The metal band cross section first rises to a maximum at a photon energy of 39 eV (electron KE of 33 eV). This is known in atomic spectroscopy as a delayed maximum[25] and arises because of the centrifugal barrier in the electronic potential of high angular momentum electrons. The effective potential experienced by an electron in an atom can be approximated by the central field potential[25] and the radial wave equation is given by:

$$\left[\frac{-d^2}{dr^2} + \frac{l(l+1)}{r^2} + V(r)\right]\Psi_{nl}(r) = E\Psi_{nl}(r)$$

where the $l(l+1)/r^2$ term is the centrifugal repulsion term. The main channel for ionization of f electrons is via a free electron g wave.[26] At low photon energies the bound f electron wave function does not have a good overlap with the continuum g electron wave because the centrifugal barrier (see Figure 6) limits core penetration, so the photoionization cross section is low. As the photon energy rises, the overlap increases and the cross section maximizes before falling because of the oscillatory nature of the outgoing electron wave function, just as in the ligand-based orbitals. Here, we see the origins of the dramatic relative intensity changes in He I/He II photoelectron spectra of uranium organometallics: the delayed maximum (39 eV) is quite close to the He II radiation energy (42 eV). The position of the delayed maximum for the f electron ionization (at 39 eV) is in good agreement with the value (electron KE 40 ± 5 eV, photon energy 46 ± 5 eV) predicted by central field calculations on uranium.[27] The bonding interactions of the 5f orbitals of uranocene seem to reduce the centrifugal barrier maximum. One possible explanation is that through bonding with the ligand e_{2u} orbitals the 5f orbitals become more diffuse. Penetration of the f electron density by the continuum wave function is then more effective at larger distances, and the height of the centrifugal barrier is reduced.

The second main feature in the f band RPPICS, found in the 90–125-eV photon energy region, is related to the photoionization of atomic uranium 5d electrons (IE = 101 and 110 eV), in a process referred to as 5d → 5f resonant photoemission.

To observe giant resonant enhancement of photoemission, three conditions must be met:

1. The excited electron must be of high angular momentum (i.e. d or f) such that it can exist in a quasi bound state above the ionization potential in the inner well region of the combined attractive coulomb and repulsive centrifugal potential.
2. The orbital the electron is being excited to must not be filled.
3. The inner and outer shell must be of the same principle quantum number to ensure a sufficiently large overlap between the two orbitals.

Around the 5d ionization energy the following absorption and emission processes can occur:

$$5d^{10}5f^n \rightarrow \underset{\text{photoabsorption}}{5d^9 5f^{n+1}} \rightarrow \underset{\text{autoionization}}{5d^9 5f^n + e^-} \quad (1)$$

$$5d^{10}5f^n \rightarrow \underset{\text{photoabsorption}}{5d^9 5f^{n+1}} \rightarrow \underset{\text{Super–Coster–Kronig (SCK) decay}}{5d^{10}5f^{n-1} + e^-} \quad (2)$$

The kinetic energy of the electron ejected in (2) is identical with that acquired by the direct photoemission process:

$$5d^{10}5f^n \rightarrow 5d^{10}5f^{n-1} + e^- \quad (3)$$

Interchannel coupling between the corresponding final states in (2) and (3) should lead to a Fano profile for the resonance.[28,29]

Two Fano resonance profiles with a constant background cross section were fitted to the experimentally determined f band RPPICS. The resonance function used was

$$\sigma = \sigma_0(q + \epsilon)^2/(1 + \epsilon^2) \qquad \epsilon = (E - E_r)/0.5W$$

where σ_0 = background cross section, E_r = resonance energy, W = resonance width, and q = line profile index. That two profiles were needed confirms the assignment of this feature to the 5d →

(23) Brennan, J. G.; Cooper, G.; Green, J. C.; Payne, M. P.; Redfern, C. M. *J. Electron Spectro. Relat. Phenom.* **1987**, *43*, 297.
(24) Heitler, W. *Quantum Theory of Radiation*; Oxford University Press: London, 1954.
(25) Cowan, R. D. *The Theory of Atomic Structure and Spectra*; Chemical Abstracts Service: Columbus, OH, 1981.
(26) Cooper, J. W.; Manson, S. T. *Phys. Rev.* **1968**, *165*, 126.
(27) Yeh, J. J.; Lindau, I. *At. Data Nucl. Data Tables* **1985**, *32*, 1.
(28) Fano, U. *Phys. Rev.* **1961**, *124*, 1866.
(29) Fano, U.; Cooper, J. W. *Phys. Rev.* **1965**, *137*, A1364.

5f resonant emission, as the separation of the two peaks (11 ± 2 eV) is comparable to the value of the spin-orbit coupling (9 eV) of the $5d^9$ configuration in the uranium atom.

The resonance profile is similar to the experimental results for the cross sections of uranium metal.[30] We note that the two spin-orbit components of the uranocene d → f resonance do not have an intensity ratio of 3:2, as might be expected for the $D_{5/2}$:$D_{3/2}$ hole states. The $D_{5/2}$ state has the lower excitation energy as the d orbitals are more than half-filled; however, it gives rise to the weaker of the two resonance peaks. This has been discussed by Wendin[31] for the 5d → 5f resonances of thorium and uranium metal. The experimental profiles have been successfully compared with those predicted by a local-density-based random-phase approximation. The spin-orbit splitting of the occupied levels needed to be included from the beginning. It was found that the coupling transfers oscillator strength and hence intensity from the $D_{5/2}$ level, which has a lower binding energy to the higher energy $D_{3/2}$ level as is also seen in our results.

e_{2u} Band. The behavior of the first ligand band RPPICS has features corresponding to those found in the f band RPPICS, confirming the assignment to the e_{2u} orbital, as, by symmetry, only the ligand-based e_{2u} orbitals can interact with the 5f orbitals of uranium (see Figure 1). The RPPICS plots of this band are shown in Figure 7 and the BRs of the e_{2u} band relative to the e_{2g} band in Figure 8; cross-section behavior of this orbital has clearly been influenced by its substantial metal character. As noted in the discussion of the ligand-based RPPICS, most carbon 2p based orbitals show a rapid falloff in cross section as photon energy is increased (Figure 3). The e_{2u} band in uranocene shows a much slower initial falloff than the e_{2g} band and responds to the delayed maximum in the metal f band cross section in that it also shows a small maximum at 39 eV. The e_{2u} band also shows a striking resonance in the 90-125-eV region. The resonance in the e_{2u} band is almost as strong as that in the metal band, indicating a large covalent contribution of the f orbitals to these ligand orbitals. Recent calculations[18,19] have put the metal contribution to these orbitals at 25-33%, and the magnitudes of the relative intensity changes shown here are in full accord with this substantial metal contribution.

e_{2g} Band. The e_{2g} orbitals cannot interact with the uranium f orbitals, and their RPPICS behavior is essentially that of ligand-based orbitals. By symmetry the e_{2g} orbitals can overlap with vacant metal 6d orbitals, and thus to interpret properly the RPPICS behavior of this band, we would need to establish the cross-section behavior of 6d electrons. Theoretical studies suggest cross-section changes between He I and He II photon energies somewhat similar to those found for H 1s orbitals,[27] though p-d resonance phenomena might be expected around 24- and 34-eV photon energy at which energies the U 6p shell ionizes.

As noted before[8] and confirmed by calculations,[18] the significantly higher IE of the e_{2g} electrons compared with the e_{2u} electrons suggests a substantial covalent interaction between the ring π orbitals and the U 6d orbitals, such that the e_{2g} orbitals lie lower in energy than the e_{2u} orbitals and are a larger source of bonding in uranocene.

Conclusions

Unequivocal assignment of the uranocene photoelectron spectrum has been obtained using synchrotron radiation. Cross-section behavior of the metal f band can be explained in atomic terms, and the intensity changes are mimicked in the first ligand (e_{2u}) band. The correspondence of identifiable features in the metal and e_{2u} band RPPICS provides conclusive spectroscopic evidence for substantial f orbital-e_{2u} covalent stabilization in the complex. The crucial role of 6d orbitals in complex stabilization is also implicit in the assignment.

Acknowledgment. We thank the staff at Daresbury Laboratory for experimental assistance, the SERC for financial support, Lady Margaret Hall, Oxford, for an EPA Cephalosporin Research Fellowship (J.G.B.) and the Dee Corp. for a studentship (C.M.R.).

Registry No. Bis([8]annulene)uranium, 1076-26-8.

(30) Cukier, M.; Dhez, P.; Gauthe, B.; Jaegle, P.; Wehenkeland, C.; Combet-Farnoux, F. *J. Phys. (Les Ulis, Fr.)* **1978**, *39*, 2315.
(31) Wendin, G. *Phys. Rev. Lett.* **1984**, *53*, 724.

An Investigation of the Decomposition of Osmium Carbonyl Clusters on Carbon Using Diffuse Reflectance Fourier Transform IR Spectroscopy

Jeremy J. Venter and M. Albert Vannice*

Contribution from the Department of Chemical Engineering, The Pennsylvania State University, University Park, Pennsylvania 16802. *Received July 25, 1988*

Abstract: The thermal decomposition of $Os_3(CO)_{12}$ has been studied for the first time by dispersing this cluster on an oxygen-free carbon support and using diffuse reflectance Fourier transform infrared spectroscopy (DRIFTS). The $Os_3(CO)_{12}$/C clusters decomposed straightforwardly in He, but transformed to $H_4Os_4(CO)_{12}$ during decarbonylation in H_2. First-order rate constants of decomposition in He or H_2 were determined for each cluster and compared to literature values for nucleophilic substitution in solution; they were found to be very similar. The activation energy of decarbonylation of $Os_3(CO)_{12}$ was near 28 kcal/mol in He, while $Os_3(CO)_{12}$ and $H_4Os_4(CO)_{12}$ had values of 30-33 kcal/mol in H_2. Chemisorption and DRIFTS measurements indicated the formation of highly dispersed metallic Os particles on carbon following decomposition at 673 K under either He or H_2. The DRIFTS spectra of CO chemisorbed on the surface of these Os crystallites showed no evidence of positive-valent Os. The turnover frequency (CO molecule/s/site) for CO hydrogenation compared favorably with that reported for reduced Os particles on oxide surfaces, and it was about 100-fold higher than the turnover frequencies associated with stabilized positive-valent Os clusters on oxide suports. The isothermal, integral heat of adsorption of CO was measured calorimetrically at 300 K and found to be 31.3 ± 1.1 kcal/mol. This study also represents part of the first successful application of an IR spectroscopic technique to characterize carbon-supported metal clusters.

Many studies on metal carbonyl clusters (MCC's) in solution and on oxide surfaces have appeared in the literature; however, we have found no investigation of the kinetics associated with the thermal decomposition of any such cluster. These clusters have been placed on a variety of support materials to prepare heterogeneous catalysts, and a number of techniques have been used

0002-7863/89/1511-2377$01.50/0